Food Chemistry 217 (2017) 373–378

Contents lists available at ScienceDirect

Food Chemistry

journal homepage: www.elsevier.com/locate/foodchem

Spectroscopy reveals that ethyl esters interact with proteins in wine

Mattia Di Gaspero [a,*,1], Paolo Ruzza [b,1], Rohanah Hussain [c], Simone Vincenzi [d], Barbara Biondi [b], Diana Gazzola [d], Giuliano Siligardi [c], Andrea Curioni [d]

[a] Department of Land, Environment, Agriculture and Forestry (TESAF), University of Padua, Viale dell'Università, 16, 35020 Legnaro (PD), Italy
[b] Institute of Biomolecular Chemistry of CNR, Padua Unit, via Marzolo, 1, 35127 Padua, Italy
[c] Diamond Light Source Ltd, Harwell Science and Innovation Campus, Didcot, Oxfordshire OX11 0DE, United Kingdom
[d] Department of Agronomy, Food, Natural Resources Animals and Environment (DAFNAE), University of Padua, Viale dell'Università, 16, 35020 Legnaro (PD), Italy

ARTICLE INFO

Article history:
Received 18 May 2016
Received in revised form 30 August 2016
Accepted 31 August 2016
Available online 2 September 2016

Keywords:
Aroma
Ethyl esters
Proteins
Spectroscopy
SRCD
VVTL1
Wine

ABSTRACT

Impairment of wine aroma after vinification is frequently associated to bentonite treatments and this can be the result of protein removal, as recently demonstrated for ethyl esters.

To evaluate the existence of an interaction between wine proteins and ethyl esters, the effects induced by these fermentative aroma compounds on the secondary structure and stability of VVTL1, a Thaumatin-like protein purified from wine, was analyzed by Synchrotron Radiation Circular Dichroism (SRCD) spectroscopy. The secondary structure of wine VVTL1 was not strongly affected by the presence of selected ethyl esters. In contrast, VVTL1 stability was slightly increased by the addition of ethyl-octanoate, -decanoate and -dodecanoate, but decreased by ethyl-hexanoate. This indicates the existence of an interaction between VVTL1 and at least some aroma compounds produced during fermentation. The data suggest that proteins removal from wine by bentonite can result in indirect removal of at least some aroma compounds associated with them.

1. Introduction

Protein haze formation is the main non-microbiological defect of white wines. Although wine is inhospitable solvent for proteins due to acidic pH, ethanol concentration and polyphenols, proteins of grape origin persist into the wine after fermentation (Waters et al., 2005). In particular, some grape pathogenesis-related (PR) proteins, including Chitinases and Thaumatin-like proteins (TLPs) have been shown to be the main components involved in haze formation (Waters, Shirley, & Williams, 1996). To remove the hazing proteins, white wines are treated with bentonite before being bottled (Waters et al., 2005). This treatment, however, while giving stability to the wine, has several drawbacks, including the impairment of aromatic compounds of wine (Van Sluyter et al., 2015). It has been demonstrated that this effect is mainly due to the direct adsorption of aromatic molecules by the bentonite clay (Lambri, Dordoni, Silva, & De Faveri, 2013; Lubbers, Charpentier, & Feuillat, 1996; Vincenzi, Panighel, Gazzola, Flamini, & Curioni, 2015). However, the removal of some ethyl esters by bentonite is increased in the presence of wine proteins, as recently demonstrated. This result suggests that these fermentative aromas could be in some way associated with those wine proteins that are removed by bentonite (Vincenzi et al., 2015) However, no direct evidence of this association has been reported to date.

Thaumatin-like proteins are the most abundant protein class present in white wines (Vincenzi, Marangon, Tolin, & Curioni, 2011). Recently, the X-ray structures of three grape TLPs have been resolved (Marangon, Van Sluyter, Waters, & Menz, 2014), displaying the presence of three domains and a cleft located between domains I and II. Domain I is formed by several β-strands; domain II is characterized by the presence of α-helix segments, while domain III comprises β-strands and small loops. The presence of disulfide bridges stabilizes these domains with a conserved spatial distribution throughout the protein. The cleft positioned between domains I and II is involved in interactions with different ligands. Ligand selectivity is due to the presence of different amino acids with acidic, neutral, or basic side-chains (Marangon et al., 2014).

To confirm the hypothesis of an interaction between esters and wine proteins (Vincenzi et al., 2015), the ability of ethyl esters to interact with a purified wine VVTL1 was investigated using fluorescence and circular dichroism spectroscopies. In particular, Synchrotron Radiation Circular Dichroism (SRCD) spectroscopy employing the Diamond B23 beamline has been used to obtain structural information about the interactions by analyzing the

* Corresponding author.
E-mail address: mattia.digaspero@studenti.unipd.it (M. Di Gaspero).
[1] These authors contribute equally to this work.

http://dx.doi.org/10.1016/j.foodchem.2016.08.133
0308-8146/

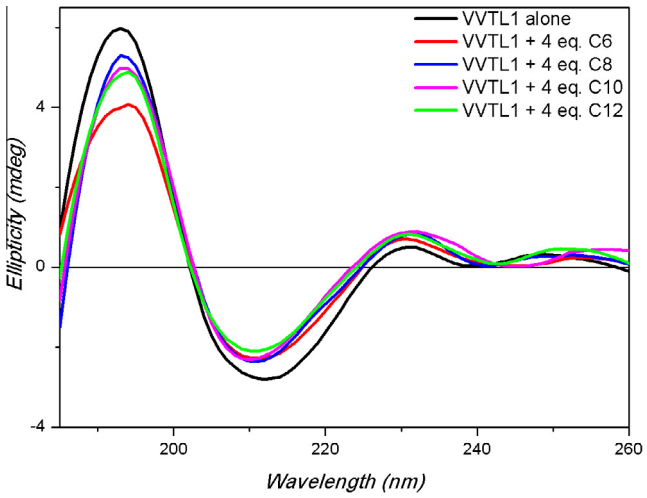

Fig. 1. Far-UV SRCD spectra of VVTL1 in model wine solution. 0.400 mg/mL of VVTL1 measured with B23 module B, in presence (4 eq.) and absence of ethyl esters. VVTL1 (black), VVTL1 + **C6** (red), VVTL1 + **C8** (blue), VVTL1 + **C10** (magenta) and VVTL1 + **C12** (green). Integration time 1 s, 0.02 cm cylindrical cell filled with 40 μL solution, monochromator slit widths 0.500 mm (1.2 nm bandwidth). (For interpretation of the references to color in this figure legend, the reader is referred to the web version of this article.)

effect of ethyl esters with different chain lengths (from C6 to C12) on the VVTL1 UV-photo and thermal stability. The high performance of the B23 beamline to detect sample perturbations in terms of sensitivity, speed, ease, and small amount of material required (Hussain, Jávorfi, & Siligardi, 2012a), enabled the investigation of ligand-binding interactions otherwise unattainable using bench top CD and NMR instruments.

2. Materials and methods

2.1. Protein purification

VVTL1 was purified from the juice of Manzoni Bianco grape provided by commercial wineries in the Conegliano area (Italy) according to a modified procedure of Van Sluyter et al., 2009. Briefly, one hundred liters of grape juice were treated with 4.0 g/L of polyvinylpolypyrrolidone (Sigma-Aldrich, Milan, Italy), 1.5 g/L of charcoal (Sigma-Aldrich), 0.6 g/L of potassium metabisulfite (Everintec, Venice, Italy) and stored overnight at 0 °C. The mixture was filtered on 0.45 μm cellulose acetate regenerated membranes (Sartorius AG, Göttingen, Germany), and then adjusted to pH 3.0 with HCl 1 M. Aliquots of 10 L were loaded on a SP-Sepharose column (2.5 × 30 cm, GE healthcare, Milan, Italy) equilibrated with 30 mM sodium citrate buffer, pH 3.0, and eluted with a gradient from 0 to 40% of 30 mM MES buffer, pH 5.0, containing 1 M NaCl in 120 min. Fractions were collected on the basis of elution profiles at 280 nm using an Akta-purifier UPC-900 (GE healthcare) and subsequently analyzed by SDS-PAGE and reverse-phase HPLC. Ammonium sulfate was added to the pooled fractions containing the desired protein to achieve a final concentration of 1.25 M. The solution was loaded on a Phenyl-Sepharose (1.5 × 20 cm) column equilibrated by two volumes of 1.25 M ammonium sulfate and 50 mM sodium citrate buffer, pH 5.0. The column was eluted with a linear gradient from 0 to 100% of 50 mM sodium citrate buffer, pH 5.0, in 120 min. The fractions containing the desired protein were collected, dialyzed against MilliQ water (3.5 kDa MWCO) and freeze dried.

Ten mg of this protein batch was further purified by semipreparative HPLC using a Shimadzu LC-8 system (Shimazdu, Kyoto, Japan) on an Jupiter C18, 10 μm, 300 Å, (250 × 10 mm) column (Phenomenex, Torrance, CA). Protein was eluted by a linear gradient from 30 to 70% of eluent B (9:1 acetonitrile-water with 0.05% TFA) in 40 min against 0.05% TFA in water (eluent A), obtaining 6.08 mg of pure VVTL1 (>99% by analytical HPLC).

Peptide mass fingerprinting analysis on trypsin digestion products using a LC MS/MS Xevo G2-S Q-TOF (Waters) mass spectrometer and Mascot software (Berndt, Hobohm, & Langen, 1999) have been used to identify the isolated VVTL1.

2.2. Synchrotron radiation circular dichroism

Ethyl decanoate (**C10**) and ethyl dodecanoate (**C12**) were purchased from Fluka (Sigma-Aldrich), ethyl hexanoate (**C6**) from B. H.D. Laboratory Chemical Division (Poole, England) and ethyl octanoate (**C8**) from Eastman Organic Chemicals (Rochester, NY).

Protein sample was prepared by dissolving 0.4 mg/mL of lyophilized VVTL1 in a model wine solution (MWS, 5 g/L of *meso*-tartaric acid and 12% ethanol adjusted to pH 3.2). The optically inactive *meso* form of tartaric acid was used to minimize the interference in the CD spectrum of the chiral form. Stock solutions of ethyl esters (0.07 mM) were prepared by dissolving the appropriate amount of each ester in MWS. SRCD spectra from 180 to 260 nm were collected at the Diamond B23 beamline module end station B using integration time of 1 s, 1 nm digital resolution and 39 nm/min scan speed. Different bandwidths (1.2–1.8 nm) were used according the different experiments. Spectra were measured using Suprasil cell (Hellma Ltd.) with 0.02 cm pathlength. Thermal stability was monitored in the 5–70 °C temperature range at 5 °C increments with 5 min equilibration time using Quantum Peltier temperature controller. Protein UV photo-denaturation was investigated by measuring twenty consecutive repeated scans for each sample at 25 °C. SRCD spectra were processed and analyzed using the CDApps software (Hussain et al., 2015).

2.3. Fluorescence measurements

Fluorescence spectra were recorded from 285 to 385 nm using a Perkin Elmer LS50B spectrofluorimeter, with the excitation and emission slit widths set at 5 nm. The excitation wavelength was 280 nm. Briefly, small microliter amounts of ethyl ester stock solutions (3.95 μM) in MWS, were added to 900 μL of VVTL1 solution in MWS, (0.021 mg/mL) in a quartz cell (1.0 cm pathlength) to achieve a ethyl ester: protein molar ratios of about 4:1.

Table 1
Secondary structure content of VVTL1 (0.400 mg/mL) with and without ethyl esters calculated using CONTINLL (Siligardi & Hussain, 2015) of CDApps (Hussain et al., 2015).

Sample	% Secondary structure				T_M (K)
	β	Turns	Unordered	α	
VVTL1	41.4	22.3	31.9	4.4	270.35; 325.95
VVTL1 + C6	43.0	21.9	30.5	4.7	322.85
VVTL1 + C8	42.8	22.3	30.7	4.2	309.25; 327.65
VVTL1 + C10	43.3	22.3	30.2	4.3	293.45; 327.95
VVTL1 + C12	43.1	21.8	30.4	4.7	298.95; 328.55

3. Results and discussion

Among the protein that "survive" the fermentation of white musts, grape TLPs are the most abundant class and this is confirmed also for the Manzoni Bianco variety here used (Berndt et al., 1999). The TLP purified from Manzoni Bianco juice was identified as the grape VVTL1 (gi: 520729528, UniProtKB: o04708), whose X-ray structure (PDB: 4L5H) and some physico-chemical parameters have been recently determined (Marangon et al., 2014).

Therefore, the relative abundance in wine and the knowledge of the molecular structure of this protein make it a good candidate for the study of the interaction between wine proteins and aroma compounds. Among the huge number of wine aromatic molecules, ethyl esters, which are produced by yeast during fermentation Po láškova, Herszage, & Ebeler, (2008) have been recently identified as those most affected by the presence of proteins during bentonite treatments to wines, suggesting that they are potentially largely involved in the interactions with protein (Vincenzi et al., 2015).

As the ethyl esters are spectroscopically transparent in the far-UV region compared to proteins, their association with VVTL1 is not easy to detect. For this reason, the effect induced by the addition of these potential ligands on the circular dichroism (CD) spectrum of VVTL1 was analyzed. CD is widely used to identify the secondary structure of protein as well as to evaluate the binding of ligands and their effects on proteins stability and structure (Siligardi & Hussain, 2015). To mimic the conditions found in wine, experiments were performed in a model wine solution at pH 3.2 containing tartaric acid and ethanol.

The far-UV SRCD spectrum of VVTL1 at 25 °C showed two positive peaks at about 195 and 230 nm attributed to the amide bond (π-π^*) and to the aromatic side-chains (La Tyr and Bb Trp bands according to Platt notation (Platt, 1949), respectively, and a negative peak at 210 nm due to the n-π^* transition of the amide bond (Fig. 1). The addition of aroma esters slightly modified the two amide bands at 195 and 210 nm, but not the positive bands at 230 nm likely associated to the aromatic side-chain π-π^* transitions (Fig. 1). From CD data, the estimation of the protein secondary structure content for VVTL1 alone and in presence of ethyl esters, was conducted using the Diamond CDApps software (Hussain et al., 2015) containing CONTIN algorithm (Sreerama & Woody, 2000). The results revealed that the apo form of VVTL1 at 25 °C was characterized by a dominating content of β-sheet, in accordance with the X-ray structure (Marangon et al., 2014). The addition of esters slightly increased the content of ordered structure (Table 1). These data suggest that the secondary structure of VVTL1 was barely affected by the presence of the ethyl esters and that the protein-aroma interaction did not involve aromatic residues as no spectral changes upon addition of ethyl esters were observed at 230 nm.

To confirm this hypothesis, the fluorescence spectrum of VVTL1 in the 300–420 nm region was measured in the absence and presence of four molar equivalents of ethyl esters. As shown in Fig. S1, Supplementary Information, the addition of ligands did not significantly alter the emission spectrum of the tryptophan, indicating that ethyl esters did not interact with the side-chain of Trp residues or modify the protein structure around these residues.

To verify that the ethyl esters are able to bind to VVTL1, both UV-photo and thermal denaturation assays were carried out. It has been reported that the high UV photon flux of B23 beamline (at Diamond Light Source, a synchrotron of third generation) can denature proteins (Hussain et al., 2012a). Indeed, a significant decrease of the amount of secondary structure upon light irradiation using the intense far-UV radiation has been observed for proteins with a significant content of α-helical and/or β-sheet structure (Clarke & Jones, 2004). Like thermal denaturation, UV denaturation varies from protein to protein, being also affected by the presence of ligands. The mechanism of photo-denaturation is likely to include free radical damage to the photosensitive tryptophan and tyrosine residues (Grosvenor, Morton, & Dyer, 2010) Experiments were conducted to check the sensitivity of the studied protein to photo-denaturation, as such phenomenon is likely to occur. This can also be used to assess the effect of both environmental parameters (solvent, detergent, pH, ...) and interactions with molecules on protein stability and to qualitatively evidence these interactions (Hussain, Jàvorfi, & Siligardi 2012b; Longo; Hussain, & Siligardi, 2015). The UV-denaturation assay was performed by measuring twenty consecutive repeated scans in the 185–260 nm far-UV region of VVTL1 in WMS in the presence of ethyl esters. An example is given Fig. 2 for ethyl-hexanoate.

By keeping constant protein concentration, volume of the solutions and instrument parameters (cell pathlength and photon flux of the irradiating incident light beam), the observed SRCD spectral changes were indicative of protein photo-denaturation effects. This was better illustrated by the plot of the SRCD intensity at single

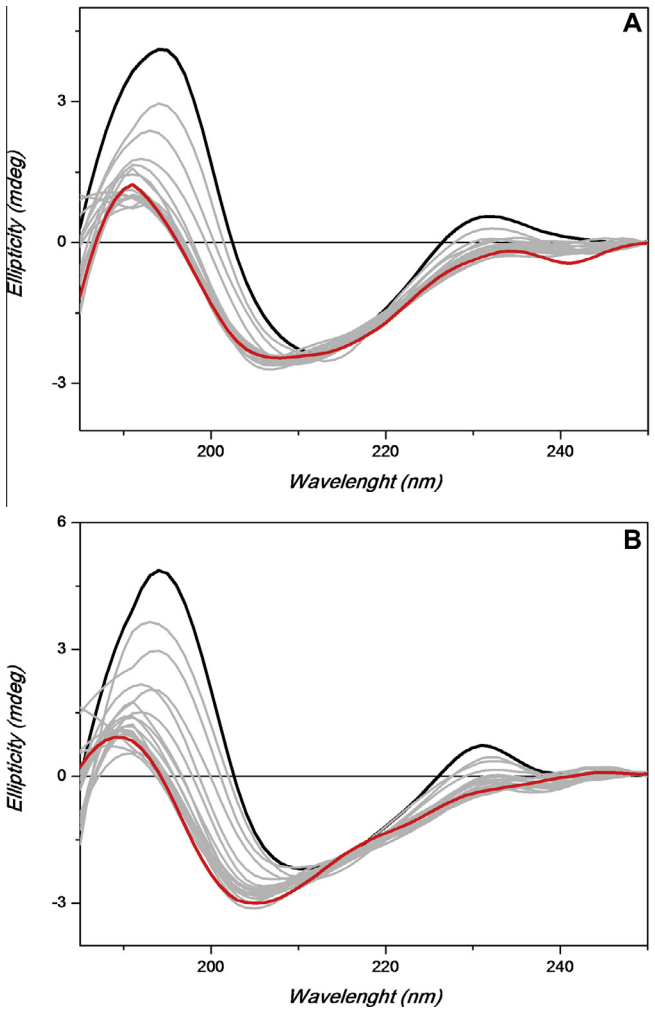

Fig. 2. (**A**) Twenty repeated consecutive SRCD scans of VVTL1 (0.400 mg/mL) in model wine, pH 3.2, measured with B23 module B. The solid black line indicates the first scan and the solid red line the 20th scan. Integration time 1 s, 0.02 cm cylindrical cell filled with 30 µl solution, monochromator slit widths 1.000 mm (2 nm bandwidth), and synchrotron ring current 268 mA. (**B**) Twenty repeated consecutive SRCD scans of VVTL1-ethyl hexanoate (0.400 mg/mL, molar ratio 1:4) in model wine, pH 3.2, measured with B23 module B under the same experimental conditions described for (**A**). (For interpretation of the references to color in this figure legend, the reader is referred to the web version of this article.)

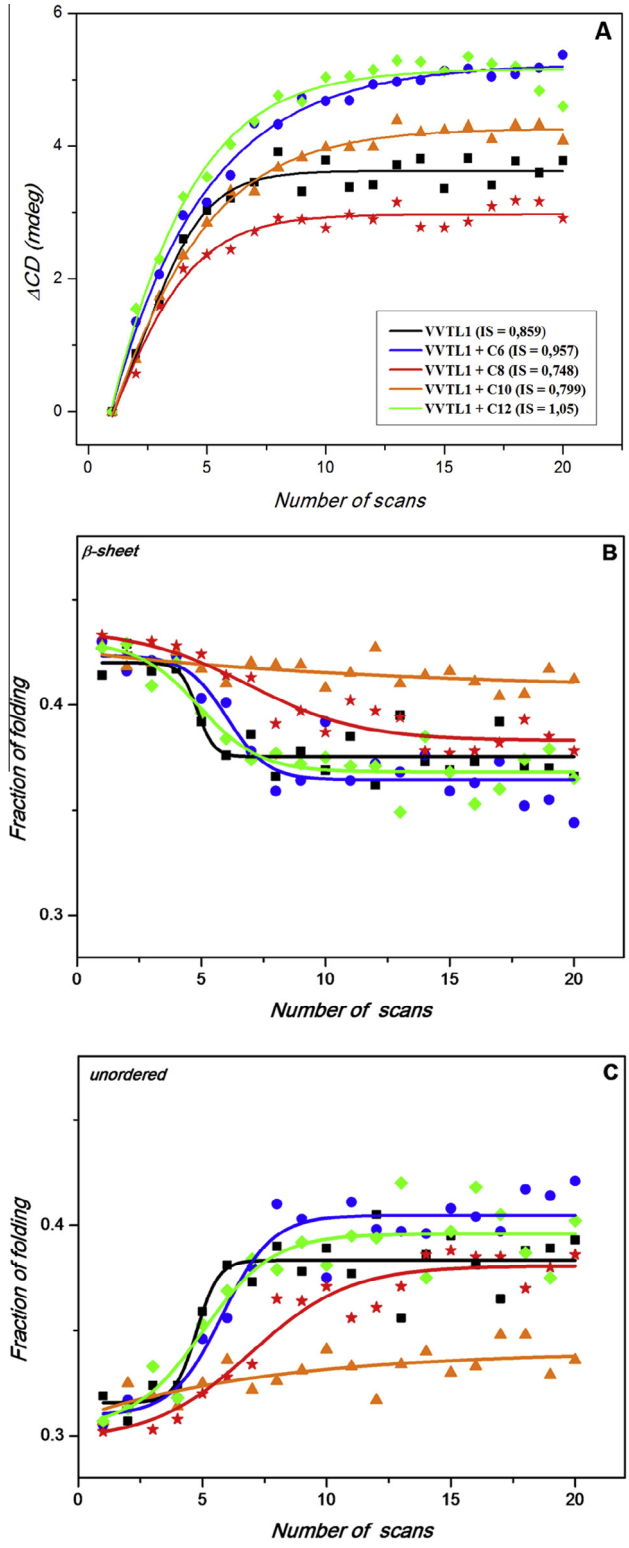

Fig. 3. (**A**) Plot of the SRCD signal at 195 nm for VVTL1 (black), VVTL1 + **C6** (blue); VVTL1 + **C8** (orange); VVTL1 + **C10** (red) and VVTL1 + **C12** (green) versus number of scans. For each sample "IS" is the value of the initial slope of the curve. (**B**) and (**C**) Plot of secondary structure content for VVTL1 (black), VVTL1 + **C6** (blue); VVTL1 + **C8** (orange); VVTL1 + **C10** (red) and VVTL1 + **C12** (green) determined with CONTINLL (Siligardi & Hussain, 2015) of CDApps (Hussain et al., 2015) from SRCD data versus number of scans. For all measurements VVTL1 concentration was 0.400 mg/mL, ethyl ester concentration was 0.07 mM, protein/ester molar ratio was 1:4. The SRCD spectra (unsmoothed) were measured using B23 module B, integration time 1 s, 1.000 mm (2 nm bandwidth) using a cylindrical Suprasil cell of 0.02 cm pathlength (Hellma) filled with 40 μl of solution. (For interpretation of the references to color in this figure legend, the reader is referred to the web version of this article.)

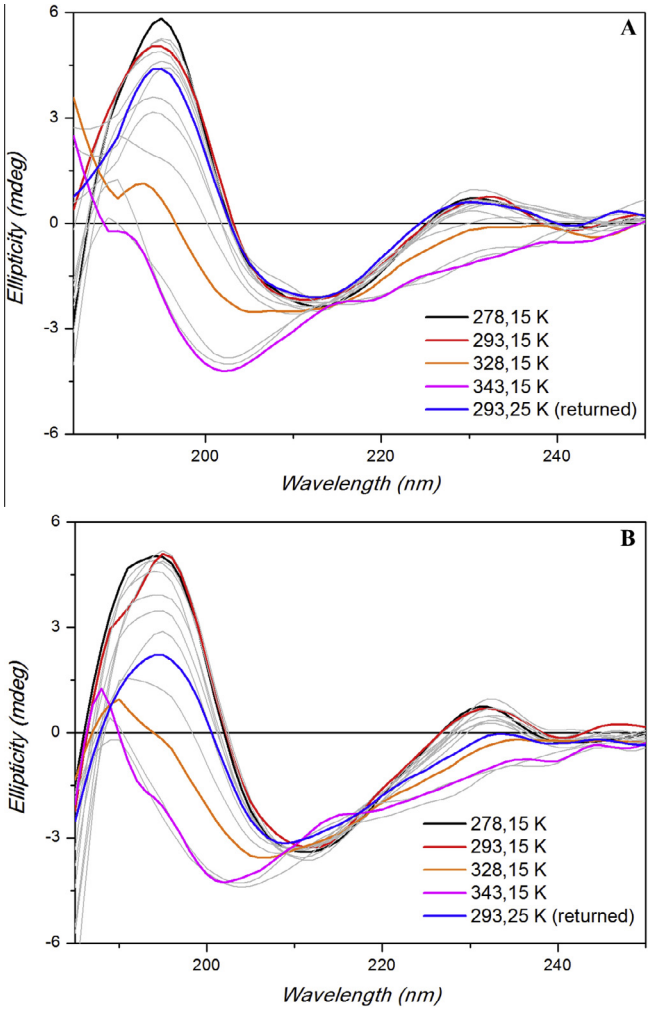

Fig. 4. (**A**) Far-UV SRCD spectra of VVTL1 in model wine measured with B23 module B at different temperatures. VVTL1 concentration was 0.400 mg/mL; integration time 1 s, 0.02 cm cylindrical cell (40 μl), monochromator slit widths 0.500 mm (1.1 nm band width (bw)) to eliminate the effect of UV denaturation. **(B)** Far-UV SRCD spectra of VVTL1 in model wine in presence of four molar equivalents of **C6** measured with B23 module B at different temperatures. VVTL1 concentration was 0.400 mg/mL; integration time 1 s, 0.02 cm cylindrical cell (40 μl), monochromator slit widths 0.500 mm (1.1 nm bw).

wavelength versus the number of scans. The fitting of the experimental data using 1st or 2nd order exponential equations (CDApps) can be seen as the relative different rates of UV-denaturation between VVTL1 with and without ligands (Fig. 3A).

The rates of UV-denaturation of the VVTL1 in the presence of ethyl esters are different from that of VVTL1 alone and this result is unambiguously indicative of an interaction between the protein and the esters. Ethyl octanoate (**C8**) appeared to increase the VVTL1 photo-stability more than the other esters (**C6**, **C10** and **C12**) with the following order: **C8** > **C10** > **C12** ≈ **C6**. This was also consistent with the estimated amount of secondary structure (β-sheet and unordered) content from each of the 20 repeated consecutive SRCD scans that were different for VVTL1-**C8** and VVTL1-**C10** complex compared to that of VVTL1 (Fig. 3B). In particular, in presence of ethyl octanoate (**C8**) a very slight UV-denaturation of VVTL1 was observed. On the other hand, in presence of **C6** ester the highest change in the secondary structure of VVTL1 was detected, suggesting that this ester may act as a negative effector for protein stability.

The temperature study of VVTL1 in the 5–70 °C temperature interval (Fig. 4A) revealed a drastic change in the SRCD spectrum

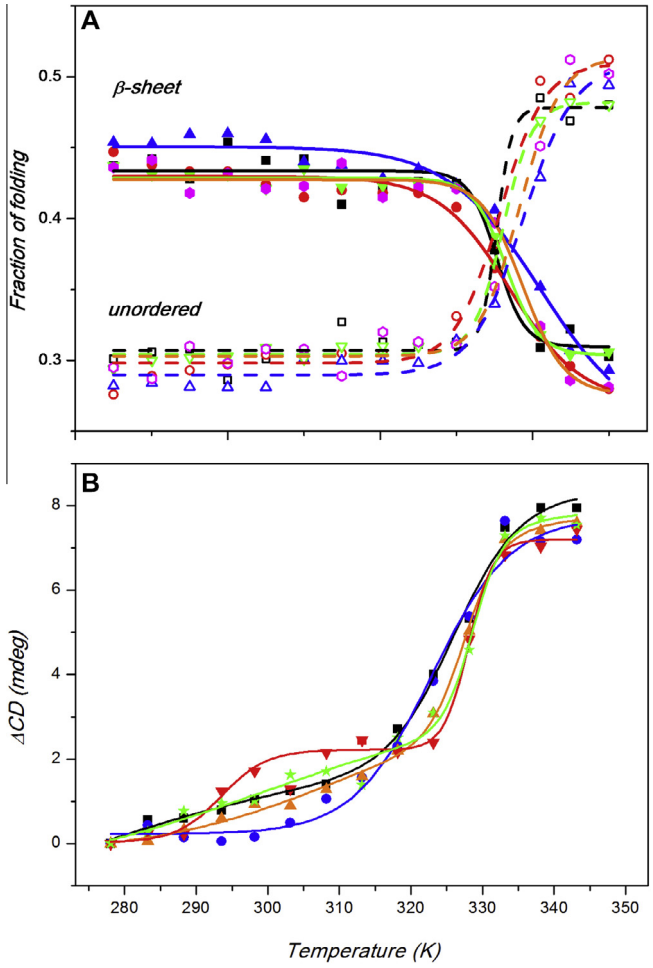

Fig. 5. (**A**) Plot of secondary structure content for VVTL1 (black), VVTL1 + **C6** (blue); VVTL1 + **C8** (orange); VVTL1 + **C10** (red) and VVTL1 + **C12** (green) determined with CONTINLL (Siligardi & Hussain, 2015) of CDApps (Hussain et al., 2015) from SRCD data versus temperature. (**B**) SRCD melting curves for VVTL1 (black), VVTL1 + **C6** (blue); VVTL1 + **C8** (orange); VVTL1 + **C10** (red) and VVTL1 + **C12** (green) obtained plotting the ellipticity at 195 nm versus temperature. For all measurements VVTL1 concentration was 0.400 mg/mL, ethyl ester concentration was 0.07 mM, protein/ester molar ratio was 1:4. The SRCD spectra (unsmoothed) were measured using B23 module B, integration time 1 s, 0.500 mm (1.2 nm bw) using a cylindrical Suprasil cell of 0.02 cm pathlength (Hellma) filled with 40 µl of solution. (For interpretation of the references to color in this figure legend, the reader is referred to the web version of this article.)

in the 55–60 °C range. In particular, the positive band at 230 nm disappeared while a negative band at about 203 nm appeared. This corresponds to a strong decrease of the β-sheet structure and subsequent increase of unordered conformation as shown in Fig. 5A. Analysis of the SRCD spectra recorded at 20 °C before and after the temperature study showed that the native VVTL1 (N) thermally treated at 70 °C (U) did not return to its native conformation N, but to a non-native conformation (N_N) with less CD intensity than that of the N protein. These data confirm previous results, which indicated partial reversibility for the (thermal) denaturation of grape TLPs (Falconer et al., 2010).

The behavior of the SRCD spectra of the VVTL1 after heating and cooling was strongly affected by the addition of ethyl ester (such as protein spectra with ethyl hexanoate reported in Fig. 5B).

In the presence of **C10**, **C12** and **C6** ethyl esters, the CD signal of the non-native conformation (N_N) further decreased in the following order: **C10** < **C12** < **C6** confirming the negative contribution of ethyl hexanoate to protein stability. On the contrary, the addition of **C8** ester increased the reversibility of the thermal denaturation process, which was consistent with the reduced susceptibility to photo denaturation observed in the UV-photo induced denaturation experiments in the presence of ethyl octanoate. As show in Fig. 5B, the melting curve of VVTL1 alone can be fitted by a double Boltzmann equation, suggesting the presence of two equilibria, with melting temperatures (T_M) of 270.35 and 325.95 K. The addition of ethyl esters modified both equilibria. In particular, the presence of the **C6** ester caused the disappearance of the first equilibrium and the melting curve was fitted by a single Boltzmann equation with T_M of 322.85 K. On the other hand, in the presence of **C8**, **C10** and **C12** esters both equilibria were retained but with an increased T_M for the first equilibrium (Table 1). These results confirm the interaction of ethyl esters with grape VVTL1, although a different effect of each ester in terms of protein-stability is highlighted.

4. Conclusions

The bentonite used for wine stabilization can directly remove some aroma compounds, thus affecting the organoleptic properties of wine (Lambri et al., 2013; Lubbers et al., 1996). However, also an indirect effect of bentonite treatments due to the removal of wine proteins, which may be complexed with aroma compounds, has been recently proposed (Vincenzi et al., 2015). The present work confirms this suggestion showing that a main wine protein, Thaumatin-like protein VVTL1, is able to bind to ethyl esters of different chain lengths. Since fermentative ethyl esters substantially contribute to the wine aroma and appear to interact with proteins, it is conceivable that their removal using bentonite could indeed alter the wine aroma negatively. Therefore, the treatment with bentonite before fermentation, in particular on the must, in which the aroma compounds produced during fermentation are absent would be preferred in order to preserve the wine quality.

Author contributions

MD, PR, GS, RH and BB carried out CD and SRCD studies. SV and DG carried out protein expression and characterization. MD, PR, GS, RH, SV designed the study, analyzed and interpreted the data. MD, PR, GS, RH, SV and AC drafted the manuscript. All authors read and approved the final manuscript.

Conflict of interest statement

The authors declare no competing financial interest.

Acknowledgments

We thank Diamond Light Source for access to the beamline B23 (SM8034) that contributed to the results presented here. The research leading to these results has received funding from the European Community's Seventh Framework Programme (FP7/2007-2013) under grant agreement n° 226716.

Appendix A. Supplementary data

Supplementary data associated with this article can be found, in the online version, at http://dx.doi.org/10.1016/j.foodchem.2016.08.133.

References

Berndt, P., Hobohm, U., & Langen, H. (1999). Reliable automatic protein identification from MATRIX-Assisted laser desorption/ionization mass spectrometric peptide fingerprints. *Electrophoresis, 20*, 3521–3526.

Clarke, D. T., & Jones, G. (2004). CD12: A new high flux beamline for ultraviolet and vacuum-ultraviolet circular dichroism on the SRS Daresbury. *Journal Synchrotron Radiation, 11*, 142–149.

Falconer, R. J., Marangon, M., Van Sluyter, S. C., Neilson, K. A., Chan, C., & Waters, E. J. (2010). Thermal stability of thaumatin-like protein, chitinase, and invertase isolated from Sauvignon blanc and Semillon juice and their role in haze formation in wine. *Journal of Agricultural and Food Chemistry, 58*, 975–980.

Grosvenor, A. J., Morton, J. D., & Dyer, J. M. (2010). Profiling of residue-level photo-oxidative damage in peptides. *Amino Acids, 39*, 285–296.

Hussain, R., Benning, K., Myatt, D., Jávorfi, T., Longo, E., Rudd, T. R., et al. (2015). CDApps: Integrated software for experimental planning and data processing at beamline B23 Diamond Light Source. *Journal Synchrotron Radiation, 22*, 465–468.

Hussain, R., Jávorfi, T., & Siligardi, G. (2012b). Circular dichroism beamline B23 at the Diamond Light Source. *Journal Synchrotron Radiation, 19*, 132–135.

Hussain, R., Jávorfi, T., & Siligardi, G. (2012a). Spectroscopic Analysis: Synchrotron Radiation Circular Dichroism. In E. M. Carreira & H. Yamamoto (Eds.), *B-23 – comprehensive chirality* (pp. 438–448). Amsterdam: Elsevier Publishing Inc.

Lambri, M., Dordoni, R., Silva, A., & De Faveri, D. M. (2013). Odor-active compound adsorption onto bentonite in a model white wine solution. *American Journal of Enology and Viticulture, 61*(2), 225–233.

Longo, E., Hussain, R., & Siligardi, G. (2015). Application of circular dichroism and magnetic circular dichroism for assessing biopharmaceuticals formulations photo-stability and small ligands binding properties. *International Journal of Pharmaceutics, 480*, 84–91.

Lubbers, S., Charpentier, C., & Feuillat, M. (1996). Etude de la retention de composés d'arôme par les bentonites en mout, vin et milieux modèles. *Vitis, 35*, 59–62.

Marangon, M., Van Sluyter, S. C., Waters, E. J., & Menz, R. I. (2014). Structure of haze forming proteins in white wines: Vitis vinifera thaumatin-like proteins. *PLoS ONE, 9*, e113757.

Platt, J. R. (1949). Classification of spectra of Cata-condensed hydrocarbons. *Journal of Chemistry and Physics, 17*, 484–495.

Polášková, P., Herszage, J., & Ebeler, E. (2008). Wine flavor: Chemistry in a glass. *Chemical Society Reviews, 37*, 2478–2489.

Siligardi, G., & Hussain, R. (2015). CD Spectroscopy: An Essential Tool for Quality Control of Protein Folding. In J. O. Raymond (Ed.), *Structural proteomics: High-throughput methods in molecular biology* (pp. 255–276). New York: Springer Publishing Inc.

Sreerama, N., & Woody, R. W. (2000). Estimation of protein secondary structure from circular dichroism spectra: Comparison of CONTIN, SELCON, and CDSSTR methods with an expanded reference set. *Analytical Biochemistry, 287*, 252–260.

Van Sluyter, S. C., Marangon, M., Stranks, S. D., Neilson, K. A., Hayasaka, Y., Haynes, P. A., et al. (2009). Two-step purification of pathogenesis-related proteins from grape juice and crystallization of thaumatin-like proteins. *Journal of Agricultural and Food Chemistry, 57*, 11376–11382.

Van Sluyter, S. C., McRae, J. M., Falconer, R. J., Smith, P. A., Bacic, A., Waters, E. J., et al. (2015). Wine protein haze: Mechanisms of formation and advances in prevention. *Journal of Agricultural and Food Chemistry, 63*, 4020–4030.

Vincenzi, S., Marangon, M., Tolin, S., & Curioni, A. (2011). Protein evolution during the early stages of white winemaking and its relations with wine stability. *Australian Journal of Grape and Wine Research, 17*, 20–27.

Vincenzi, S., Panighel, A., Gazzola, D., Flamini, R., & Curioni, A. (2015). Study of combined effect of proteins and bentonite fining on the wine aroma loss. *Journal of Agricultural and Food Chemistry, 63*, 2314–2320.

Waters, E. J., Alexander, G., Muhlack, R., Pocock, K. F., Colby, C., O'Neill, B. K., et al. (2005). Preventing protein haze in bottled white wine. *Australian Journal of Grape and Wine Research, 11*, 215–225.

Waters, E. J., Shirley, N. J., & Williams, P. J. (1996). Nuisance proteins of wine are grape pathogenesis-related proteins. *Journal of Agricultural and Food Chemistry, 44*, 3–5.